LiNbO₃-Tm³⁺ Crystal. Material for Optical Cooling

Ninel Kokanyan [1,2,*], Nune Mkhitaryan [3], Gagik Demirkhanyan [3,4], Ajith Kumar [5], Michel Aillerie [2], Dhiraj Sardar [5] and Edvard Kokanyan [3,4]

[1] Chaire Photonique, LMOPS, CentraleSupélec, 2 rue Edouard Belin, 57220 Metz, France
[2] Université de Lorraine, LMOPS, 2 rue Edouard Belin, 57070 Metz, France; michel.aillerie@univ-lorraine.fr
[3] Armenian State Pedagogical University after Kh. Abovyan, TigranMetsi Ave., 17, Yerevan 0010, Armenia; nune.leo.nm@gmail.com (N.M.); gdemirkhanyan@gmail.com (G.D.); edvardkokanyan@gmail.com (E.K.)
[4] Institute for Physical Research, National Academy of Sciences of Armenia, Ashtarak-2 0203, Armenia
[5] Department of Physics and Astronomy, The University of Texas at San Antonio, San Antonio, TX 78249, USA; akgsh2005@gmail.com (A.K.); Dsardar@utsa.edu (D.S.)
* Correspondence: ninel.kokanyan@centralesupelec.fr

Abstract: The possibilities of LiNbO₃-Tm³⁺ crystals for optical cooling based on anti-Stokes luminescence in the wavelength range of 1818–2200 nm are investigated. The concentration dependences of the final temperature of the crystal have been determined under continuous (CW) excitation at wavelengths of 1822–1977 nm with a pump intensity $F_p = 5 \times 10^{21}$ cm⁻²s⁻¹. It was shown that significant cooling with ΔT = 22 K, 19 K, and 16.4 K can be achieved, respectively, with excitation at wavelengths 1977, 1967, and 1948 nm.

Keywords: Lithium Niobate crystals; optical cooling; rare-earth ions

1. Introduction

Lithium Niobate crystals, LiNbO₃ (LN), doped with trivalent rare earth ions (RE³⁺), are good materials for small-sized multifunctional lasers in the infrared and visible spectral regions [1,2]. These crystals can be promising for optical cooling based on anti-Stokes radiation (ASL) of impurity ions, as well as for creating self-cooling lasers [3–6]. In [7], the possibilities of an LN-Ho crystal for optical cooling were studied. In [5] is given a review of studies on the cooling capabilities of crystalline (KGd(WO₄)₂, KY(WO₄)₂, YAG, Y₂SiO₅, YLF, etc.) and amorphous (ZBLANP, ZBLANP, BIG etc.) materials doped with Yb³⁺, Er³⁺ and Tm³⁺ ions.

The optical spectra of impurity absorption and radiation of the LN: Tm³⁺ crystal in the 600–2000 nm wavelength region were studied in [8,9]. In particular, in [8], the standard Judd-Ofelt analysis of the absorption spectra from the ³H₆ ground-state manifold is carried out and the intensity parameters are defined: $\Omega_2 = 6.29 \times 10^{-20}$, $\Omega_4 = 0.54 \times 10^{-20}$ and $\Omega_6 = 0.79 \times 10^{-20}$ cm². The energy levels scheme of ground, ³H₆, and first exited, ³F₄, manifolds of Tm³⁺ ion in LN is given on Figure 1. The main spectroscopic parameters with taking into account the transitions between Stark sublevels of ³H₆ and ³F₄ are calculated in [9].

In this work, based on an analysis of the energy scheme of Stark levels and the results of calculations of spectroscopic parameters, we consider the possibilities of an LN-Tm³⁺ crystal for optical cooling based on ASL in the wavelength range 1818–2000 nm.
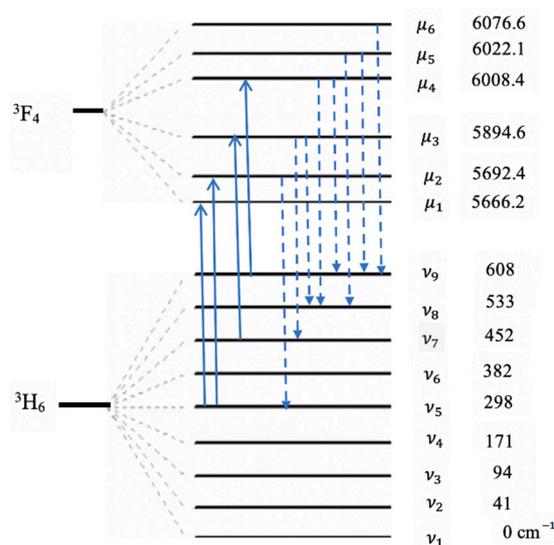
Figure 1. Energy levels scheme of $^3H_6$ and $^3F_4$ manifolds Tm^{3+} ion in LN [9].

2. Possibilities of Using the LN-Tm^{3+} Crystal in Optical Cooling Systems

The absorption and luminescence spectra of the LN-Tm^{3+} crystal at $N_{Tm} = 2 \times 10^{20}$ cm^{-3} (N_{Tm} is concentration of impurity Tm^{3+} ions) in the wavelength range of 1600–2000 nm at room temperature are shown in Figure 2. Luminescence measurements of the samples were done by using Quanta Master 51 spectrofluorometer (Photon Technology International Inc. NJ, USA) with an InGaAs detector for NIR (Teledyne Judson Technologies, 062-8451, Mongomeryville, PA, USA) and PMT (Hamamatzu, NJ, USA) for the visible emission. Excitation sources used are 800 nm power tunable fiber coupled Fabry Perot continuous laser diode (Thorlab, Model LM14S2, NJ, USA). For laser excitation the spot size was about 3 mm at an excitation power of 500 mW. Absorption measurements were carried out using Cary 500 UV-VIS-NIR network spectrometer with 0.1 nm resolution.

As it is known, optical cooling is caused by anti-Stokes luminescence (ASL) at wavelengths satisfying the following condition

$$\lambda_{ex} > \lambda_{ASL} > \lambda_f, \tag{1}$$

where λ_{ex} is the excitation wavelength and $\left\langle \lambda_f \right\rangle$—is the average luminescence wavelength defined by the formula below:

$$\lambda_f = \int_0^\infty \lambda I_f(\lambda) d\lambda \Big/ \int_0^\infty I_f(\lambda) d\lambda$$

($I_f(\lambda)$—is the spectral density of the luminescence intensity). According to the emission spectrum, we obtain: $\lambda_f = 1818.6$ nm (Figure 2). Condition (1) limits the set of wavelengths of both excitation and ASL. Thus, analysis of the absorption spectrum shows that, to gain optical cooling, excitations at wavelengths in the range 1822–1977 nm are possible. A study of the energy scheme shows that, in the indicated wavelength range, spectral absorption lines can be induced by the 17 inter-Stark transitions. The spectroscopic parameters of the corresponding spectral absorption lines are given in Table 1. The values of the absorption efficiency, determined by the formula

$$\xi_{abs}(i \to f) = \frac{\alpha_{i,f} exp\left(-\frac{\varepsilon_i - \varepsilon_1}{KT}\right)}{\sum_{j,m} \alpha_{j,m} exp\left(-\frac{\varepsilon_i - \varepsilon_1}{KT}\right)}, \tag{2}$$

where $\alpha_{i,f}$—is the integral absorption coefficient at the transition $i \to f$, ε_j is the energy of the j-th Stark state of the main manifold, K is the Boltzmann constant, T is the temperature.
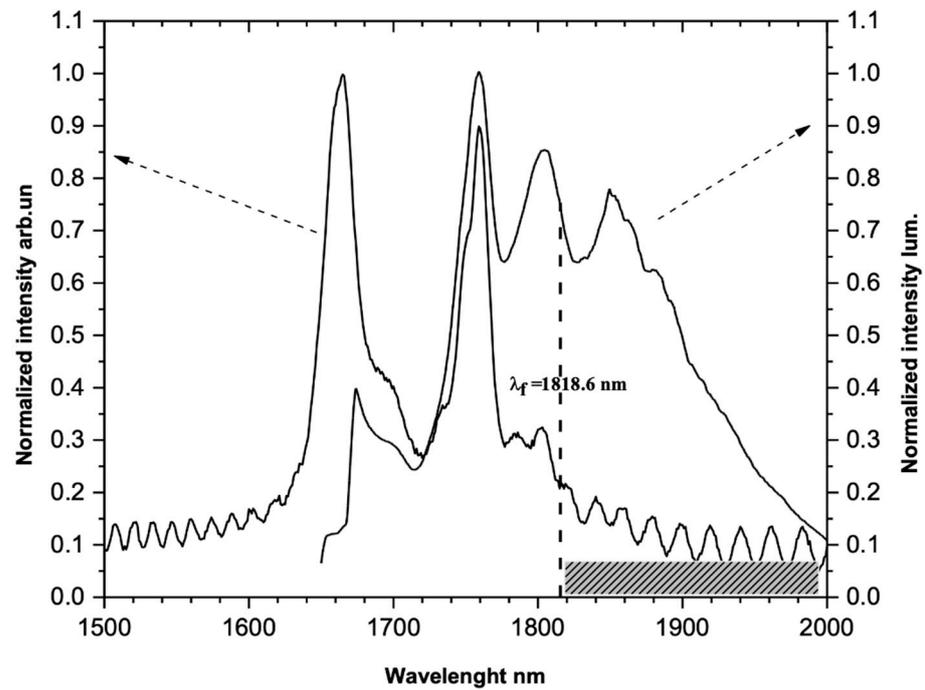
Figure 2. Absorption and luminescence normalized spectra.

Table 1. Spectroscopic parameters of the corresponding spectral absorption lines.

λ_{ex}, nm	Transition	[1] S, 10^{-21} cm^2	[2] α, 10^{-26} cm^3	[3] N_i/N_0	[4] σ_p, 10^{-20} cm^2	[5] ξ_{abs}, 10^{-3}%
1822	$\nu_8 \rightarrow \mu_5$	0.9298	0.087	0.022	0.174	1.0
1826	$\nu_8 \rightarrow \mu_4$	1.1059	0.104	0.022	0.208	1.2
1829	$\nu_9 \rightarrow \mu_6$	0.1143	0.007	0.015	0.014	0.1
1837	$\nu_7 \rightarrow \mu_3$	0.1695	0.024	0.032	0.048	0.4
1847	$\nu_9 \rightarrow \mu_5$	0.0831	0.005	0.015	0.001	<0.1
1852	$\nu_9 \rightarrow \mu_4$	0.8259	0.048	0.015	0.096	0.4
1854	$\nu_5 \rightarrow \mu_2$	0.7892	0.232	0.068	0.464	8.4
1863	$\nu_5 \rightarrow \mu_1$	0.1627	0.048	0.068	0.096	1.7
1865	$\nu_8 \rightarrow \mu_3$	0.3191	0.031	0.022	0.062	0.4
1883	$\nu_6 \rightarrow \mu_2$	1.0080	0.201	0.045	0.402	4.8
1892	$\nu_6 \rightarrow \mu_1$	0.8978	0.180	0.045	0.306	4.3
1908	$\nu_7 \rightarrow \mu_2$	0.3850	0.056	0.032	0.112	1.0
1918	$\nu_7 \rightarrow \mu_1$	0.0938	0.014	0.032	0.028	0.2
1938	$\nu_8 \rightarrow \mu_2$	1.5134	0.150	0.022	0.048	1.8
1948	$\nu_8 \rightarrow \mu_1$	1.6029	0.160	0.022	0.320	1.9
1967	$\nu_9 \rightarrow \mu_2$	1.0154	0.071	0.015	0.142	0.6
1977	$\nu_9 \rightarrow \mu_1$	0.9514	0.049	0.015	0.098	0.5

[1] S is line strength; [2] α is absorption coefficient; [3] N_i/N_0 is relative population of initial level; [4] σ_p is the cross section of the excitation transition; [5] ξ_{abs} is absorption efficiency.

The spectroscopic characteristics of the ASL spectrum at room temperature in the wavelength range of 1820–2000 nm are given in Table 2.

Table 2. Spectroscopic characteristics of the anti-Stokes Luminescence (ASL) spectrum at room temperature.

Transition	λ_{em}, nm	[1] S, 10^{-21} cm^2	[2] A, s^{-1}	[3] Ni/N_0	[4] β, %
$\mu_1 \to \nu_4$	1820	0.1191	17.5	0.367	0.60
$\mu_5 \to \nu_8$	1822	0.9298	136.3	0.065	0.85
$\mu_4 \to \nu_8$	1826	1.1059	161.0	0.071	1.07
$\mu_6 \to \nu_9$	1829	0.1143	16.6	0.051	0.08
$\mu_3 \to \nu_7$	1837	0.1695	24.3	0.123	0.28
$\mu_5 \to \nu_9$	1847	0.0831	11.7	0.065	0.07
$\mu_4 \to \nu_9$	1852	0.7259	101.3	0.071	0.67
$\mu_2 \to \nu_5$	1854	0.7892	109.8	0.323	3.32
$\mu_1 \to \nu_5$	1863	0.1627	22.3	0.367	0.77
$\mu_3 \to \nu_8$	1865	0.3191	43.6	0.123	0.05
$\mu_2 \to \nu_6$	1883	1.0080	133.8	0.323	4.05
$\mu_1 \to \nu_6$	1892	0.8978	117.5	0.367	4.30
$\mu_3 \to \nu_9$	1892	0.0324	4.2	0.123	0.05
$\mu_2 \to \nu_7$	1908	0.3850	49.1	0.323	1.49
$\mu_1 \to \nu_7$	1918	0.0938	11.8	0.367	0.41
$\mu_2 \to \nu_8$	1938	1.5134	184.3	0.323	5.58
$\mu_1 \to \nu_8$	1948	1.6029	192.2	0.367	6.60
$\mu_2 \to \nu_9$	1967	1.0154	118.3	0.323	3.58

[1] S is line strength; [2] A is probability of spontaneous transitions; [3] N_i/N_0 is relative population of initial level; [4] β is luminescence branching ratio.

It has to be noted that excitation at a given wavelength can initiate ASL at several wavelengths satisfying condition (1). So, when excited at a wavelength of 1837 nm, ASL is possible at wavelengths of 1820, 1822, 1826, and 1829 nm. The set of ASL wavelengths satisfying condition (1) at a fixed excitation wavelength is given in Table 3. The cooling efficiency at a given excitation wavelength is estimated by the formula [10]

$$\gamma = \eta \left[1 - e^{-(\alpha_{ab} - \alpha_{ph})L} \right] \frac{\lambda_{ex} - \lambda_f}{\lambda_f}, \tag{3}$$

where η is quantum yield of luminescence from the excited level, α_{ab} is the radiation absorption coefficient at the wavelength λ_{ex}, α_{ph} is the background absorption coefficient of the crystal matrix, L is the length of the crystal along the optical excitation.

We notice that the probability of a non-radiative intra-center multi-phonon transition from a $^3F_4$ manifold is negligible, so that the lifetime of an excited manifold is due to radiative transitions. It can be assumed that the quantum yield of luminescence from the Stark level of the excited manifold coincides with the branching coefficient of luminescence. The $\alpha_{ab}(\lambda)$ absorption coefficient in (3) is related to the integral absorption coefficient by the relation $\alpha_{ab} = N_{Tm} \sum \left(\alpha_{i,f} / \Delta\lambda_{i \to f} \right)$, ($N_{Tm}$—is the concentration of impurity ions, $\Delta\lambda_{i \to f}$ is the width of the corresponding spectral absorption line, the summation is performed over all transitions corresponding to a given wavelength).

Considering also that the intensity of the exciting radiation is sufficiently small, so that the system is far from saturation. Then, assuming L = 0.5 cm and $\alpha_{ph} = 0.01$ cm^{-1} [6], according to Tables 1 and 2, we estimate the value γ for various transitions inducing ASL at each excitation wavelength.

Table 3. Set of ASL wavelengths satisfying condition (1) at a fixed excitation wavelength.

ASL		$\gamma_{\mu_i\to\vartheta_j}(\lambda_{ex})$, 10^{-3} % (λ_{ex}, nm)							
λ_{ASL}, nm	Transition	(1822)	(1826)	(1829)	(1837)	(1847)	(1852)	(1854)	(1863)
1820	$\mu_1\to\nu_4$	0.231	0.589	0.082	0.394	0.178	1.332	5.528	1.770
1822	$\mu_5\to\nu_8$	-	0.632	0.088	3.174	1.263	1.429	5.948	1.902
1826	$\mu_4\to\nu_8$	-	-	0.111	0.534	0.241	1.801	7.488	2.395
1829	$\mu_6\to\nu_9$	-	-	-	0.040	0.018	0.135	0.560	0.179
1837	$\mu_3\to\nu_7$	-	-	-	-	0.063	0.471	1.959	0.627
1847	$\mu_5\to\nu_9$	-	-	-	-	-	0.118	0.490	0.157
1852	$\mu_4\to\nu_9$	-	-	-	-	-	-	4.689	1.500
1854	$\mu_2\to\nu_5$	-	-	-	-	-	-	-	7.431
$\gamma_{tot}(\lambda_{ex})$, 10^{-3} %		0.231	1.221	0.281	4.142	1.763	5.286	26.662	15.961

ASL		$\gamma_{\mu_i\to\vartheta_j}(\lambda_{ex})$, 10^{-3} % (λ_{ASL}, nm)								
λ_{ASL}, nm	Transition	(1865)	(1883)	(1892)	(1908)	(1918)	(1938)	(1948)	(1967)	(1977)
1820	$\mu_1\to\nu_4$	1.247	8.970	9.343	4.092	1.343	1.709	1.961	8.506	14.552
1822	$\mu_5\to\nu_8$	1.341	9.652	10.053	4.403	1.445	1.839	2.104	9.152	15.657
1826	$\mu_4\to\nu_8$	1.689	12.151	12.654	5.543	1.819	2.314	2.644	11.521	19.757
1829	$\mu_6\to\nu_9$	0.126	0.908	0.946	0.414	0.136	0.173	0.045	0.861	1.474
1837	$\mu_3\to\nu_7$	0.442	3.180	3.311	1.450	0.476	0.606	0.693	3.015	5.156
1847	$\mu_5\to\nu_9$	0.110	0.795	0.828	0.363	0.119	0.151	0.173	0.754	1.289
1852	$\mu_4\to\nu_9$	1.057	7.608	7.924	3.471	1.139	1.449	1.656	7.214	12.341
1854	$\mu_2\to\nu_5$	5.239	37.701	39.264	17.198	5.645	7.181	8.205	35.746	61.155
1863	$\mu_1\to\nu_5$	1.215	8.744	9.106	3.989	1.309	1.666	1.903	8.290	14.184
1865	$\mu_3\to\nu_8$	-	0.568	0.591	0.259	0.085	0.108	0.124	0.538	0.921
1883	$\mu_2\to\nu_6$	-	-	47.897	20.980	6.886	8.760	10.009	43.606	74.601
1892	$\mu_1\to\nu_6$	-	-	-	20.876	6.851	8.717	9.960	43.390	74.233
1892	$\mu_3\to\nu_9$	-	-	-	0.259	0.085	0.108	0.124	0.538	0.921
1908	$\mu_2\to\nu_7$	-	-	-	-	2.533	3.222	3.682	16.043	27.446
1918	$\mu_1\to\nu_7$	-	-	-	-	-	0.887	1.013	4.414	7.552
1938	$\mu_2\to\nu_8$	-	-	-	-	-	-	13.790	60.079	102.784
1948	$\mu_1\to\nu_8$	-	-	-	-	-	-	-	71.061	121.572
1967	$\mu_2\to\nu_9$	-	-	-	-	-	-	-	-	65.944
$\gamma_{tot}(\lambda_{ex})$, 10^{-3}%		12.466	90.277	141.917	83.297	29.871	38.89	58.086	324.728	621.539

Moreover, it should be noted that for a given excitation, ASL processes at several wavelengths satisfying condition (1) are permissible. Considering that ASL-inducing transitions are mutually independent, according to Table 3, it is easy to evaluate the cooling efficiency for each excitation wavelength: $\gamma_{tot}(\lambda_{ex}) = \sum \gamma_i(\lambda_{ex})$ (the summation is carried out over all admissible ASL channels at a given excitation wavelength). The results are shown in Table 3. It can be noticed that excitations at the wavelengths of 1883, 1892, 1908, 1938, 1948, 1967, and 1977 are the most effective.

To estimate the cooling temperature, $\Delta T = T_0 - T$, we start from the energy balance equation $E_{ph}(T_0) - E_{ph}(T) = \varepsilon(T_0)$ ($E_{ph}(T)$ is the vibrational energy of the crystal at temperature T and $\varepsilon(T_0)$ is the thermal energy absorbed in result of ASL). The latter, using the Debye approximation for lattice vibrations, can be represented as

$$\left(\frac{T_0}{T_D}\right)^4 \int_0^{T_D/T_0} \frac{x^3 dx}{e^x - 1} - \left(\frac{T}{T_D}\right)^4 \int_0^{T_D/T} \frac{x^3 dx}{e^x - 1} = \frac{N_0}{N} \times \frac{hc}{9kT_D} \times \frac{1}{1 + \tau F_p \sigma_p} \left[\tau F_p \sigma_p \sum_i \frac{\delta_L(i)}{\lambda_L(i)} - \frac{\delta_p}{\lambda_{ex}}\right], \qquad (4)$$

where N is the concentration of atoms in the matrix of the crystal LN, T_D is the Debye temperature, T_0 is the initial temperature of the crystal, δ_p and δ_L—the Boltzmann factors determining the populations of the initial Stark levels from which the processes of absorption and luminescence occur, h is the Planck constant, c is the speed of light, τ is the lifetime of the level $^3F_4$ and F_p is the photon flux density of the exciting radiation, σ_p is the cross section of the excitation transition, the summation on the right-hand side of (4) is carried out over all ASL channels, satisfying condition (1) for a given excitation wavelength. Equation (4) determines the functional dependence of the cooling temperature on the concentration of N_{Tm} impurity ions, wavelength (λ_{ex}), and excitation intensity (F_p).

The first integral on the right-hand side of (4) is easily calculated: $I(T_0) = 0.100862$ at $T_D = 503$ K and $T_0 = 300$ K. After non-complex transformations (taking into account $T < T_D$), the second integral can be transformed to the form:

$$\int_0^{T_D/T} \frac{x^3 dx}{e^x - 1} = \frac{\pi^4}{15} - \sum_{n=0}^{\infty} \frac{e^{-(n+1)\times\frac{T_D}{T}}}{(n+1)^4} \times Q_n\left(\frac{T_D}{T}\right), \tag{5}$$

where $Q_n(x) = (n+1)^3 x^3 + 3(n+1)^2 x^2 + 6(n+1)x + 6$.

Thus, Equation (4) takes the form:

$$\left(\frac{T}{T_D}\right)^4 \times \left\{ \frac{\pi^4}{15} - \sum_{n=0}^{\infty} \frac{e^{-(n+1)\times\frac{T_D}{T}}}{(n+1)^4} \times Q_n\left(\frac{T_D}{T}\right) \right\} = 0.100862 - b(\lambda_{ex}, \rho, T), \tag{6}$$

where $\rho = N_{Tm}/N$ ($N = 3.14 \times 10^{22}$ cm^{-3} is the concentration of atoms in the matrix of the crystal LN). Solving Equation (6), we determine the cooling temperature T and $\Delta T = T_0 - T$. Note that the cooling value, ΔT, depends on the cross section and the population of the initial transition level that induces absorption, as well as the number of ASLs initiated. Figure 3 shows the concentration dependences of the cooling temperature at the excitation intensity $F_p = 5 \times 10^{21}$ cm^{-2}s^{-1} at wavelengths leading to the most efficient cooling. The temperature values $\Delta T = T_0 - T$ for $N_{Tm} = 2 \times 10^{20}$ cm^{-3} are given in Table 4.
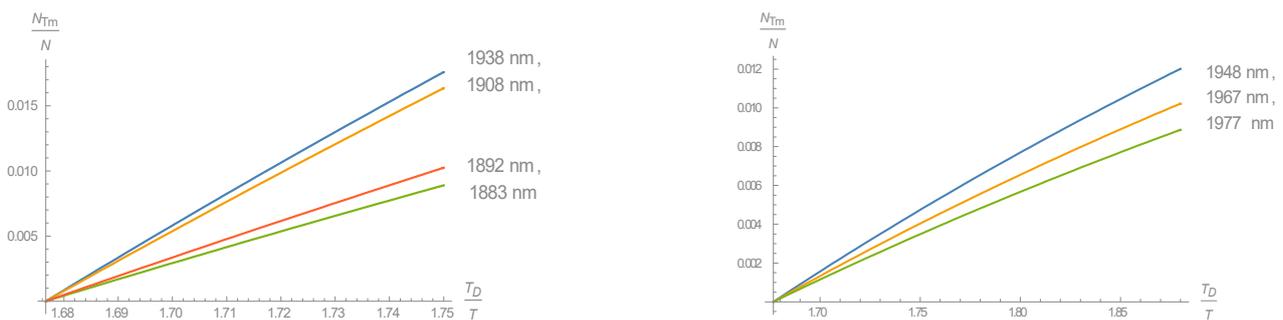
Figure 3. Concentration dependences of the cooling temperature at the excitation intensity $F_p = 5 \times 10^{21}$ cm^{-2}s^{-1} at wavelengths leading to the most efficient cooling.

Table 4. Temperature values $\Delta T = T_0 - T$ for $N_{Tm} = 2 \times 10^{20}$ cm^{-3}.

λ_{ex}, nm	ΔT, K
1822	1.7
1826	2.4
1829	0.2
1837	0.2
1847	0.3
1852	3.3
1854	3.0
1863	0.3
1865	2.6
1883	8.7
1892	8.3
1908	4.8
1918	1.0
1938	4.2
1948	16.4
1967	19.0
1977	22.0

3. Conclusions

CW excitation with intensity $F_p = 5 \times 10^{21}$ cm^{-2}s^{-1} at wavelengths in the 1822–1977 nm regions, involving multiple channels of ASL, leads to efficient cooling. At the same time, significant cooling (22 K, 19 K and 16.4 K) can be achieved with excitation at wavelengths 1977 nm, 1967 nm and 1948 nm. This is evidently due to the fact that, upon excitation at these wavelengths, a larger number of ASL channels starting from the lower levels of the $^3F_4$ manifold are involved in the cooling process.

Note that in the case of the BaY$_2$F$_8$-Tm^{3+} and KPb$_2$Cl$_5$-Er^{3+} crystals for the cooling temperature were obtained the values $\Delta T = 3.2$ K and $\Delta T = 0.12$ K, respectively [5]. In [11], for the BaY$_2$F$_8$-Tm^{3+} crystal upon excitation at a wavelength of 1855 nm was obtained the value $\Delta T = 4.8$ K [11]. In LN-Ho^{3+} crystals under CW excitations at 2035 nm and 2071 nm, for maximum cooling, temperatures were obtained $\Delta T = 2.5$ K and $\Delta T = 10.9$ K, respectively [7].

Thus, a comparison of the results obtained with the cooling properties of crystals doped with rare-earth ions with an energy level structure similar to the energy scheme of the Tm^{3+} ion shows that LN-Tm^{3+} crystal with concentration of impurity ions $N_{Tm} = 2 \times 10^{20}$ cm^{-3} is a quite promising material for systems optical cooling based on ASL.

It should be noted that the efficiency of optical cooling based on ASL of a uniaxial LN crystal can be corrected by the polarization characteristics of the absorption and emission spectra.

References

1. Cordova-Plaza, A.; Digonnet, M.; Shaw, H.J. Miniature CW and active internally Q-switched Nd: MgO:LiNbO$_3$ lasers. *IEEE J. Quantum Electron.* **1987**, *23*, 262–266. [CrossRef]
2. Lallier, E.; Pocholle, J.P.; Papuchon, M.; de Micheli, M.; Li, M.J.; He, Q.; Ostrowsky, D.B.; Grezes-Besset, C.; Pelletier, E. Nd:MgO:LiNbO$_3$ waveguide laser and amplifier. *Opt. Lett.* **1990**, *15*, 682–684. [PubMed]
3. Ruan, X.L.; Kaviany, M. Enhanced laser cooling rare-earth-ion-doped nanocrystalline powder. *Phys. Rev. B* **2006**, *73*, 155422. [CrossRef]
4. Garcia-Adeva, A.J.; Balda, R.; Fernandez, J. Upconversion cooling Er-doped low-phonon fluorescent solids. *Phys. Rev. B* **2009**, *79*, 033110. [CrossRef]
5. Nemova, G.; Kashyap, R. Laser cooling of solids. *Rep. Prog. Phys.* **2010**, *73*, 086501. [CrossRef]
6. Babajanyan, V.G. Spectroscopic study of the expected optical cooling effect of LiNbO$_3$:Er^{3+} crystal. *Laser Phys.* **2013**, *23*, 126002. [CrossRef]
7. Demirkhanyan, G.G.; Kokanyan, E.P.; Demirkhanyan, H.G.; Sardar, D.; Aillerie, M. Crystal LiNbO$_3$-Ho^{3+}: Material for optical cooling. *J. Contemp. Phys. (Armen. Acad. Sci.)* **2016**, *51*, 28–34. [CrossRef]
8. Zhang, R.; Li, H.; Zhang, P.; Hang, Y.; Xu, J. Efficient 1856nm emission from Tm,Mg:LiNbO$_3$ laser. *Opt. Express* **2013**, *21*, 020990–020998. [CrossRef] [PubMed]
9. Kokanyan, E.P.; Demirkhanyana, G.G.; Demirkhanyan, H.G. Spectroscopic properties of LiNbO$_3$:Tm^{3+} crystal in the 1650-1970nm wavelength range. *J. Contem. Phys. (Armen. Acad. Sci.)* **2018**, *53*, 227–233. [CrossRef]

10. Melgard, S.D.; Seletskiy, D.V.; Di Lieto, A.; Tonelli, M.; Sheik-Bahae, M. Optical refrigeration to 119K, below national institute of standards and technology cryogenic temperature. *Opt. Lett.* **2013**, *38*, 1588–1590. [CrossRef] [PubMed]

11. Patterson, W.; Bigotta, S.; Sheik-Bahae, M.; Parisi, D.; Tonelli, M.; Epstein, R. Anti-Stokes luminescence cooling of Tm^{3+} doped BaY_2F_8. *Opt. Express* **2008**, *16*, 1704–1710. [CrossRef] [PubMed]